

BEHAVIOUR OF FRP-SANDWICH STRUCTURES FOR LIGHTWEIGHT COMPOSITE SPRINGS IN STATIC AND CYCLIC TORSIONAL LOAD CASES

Petrich, Martin; Weimann, Tom-Luis; Thein, Ludwig; Kletzin, Ulf
TU Ilmenau, Department of Mechanical Engineering, Machine Elements Group

ABSTRACT

Fiber-reinforced polymers (FRP) are established as high-tech materials for special purposes such as racing cars, planes or bicycles. Nowadays, they are increasingly used for functional parts and machine elements. For lightweight optimization, FRP sandwich structures can be used, which also appear to be suitable for spring applications. But material data availability is often limited for UD-specimen or specific load cases, which makes it difficult to use FRPs for technical springs. In order to reduce this gap and to facilitate the development of new applications, this paper deals with the basic static and cyclic behavior of FRP sandwich strips under torsional load. Therefore, manufacturing methods have been developed, to produce FRP strip specimens with GFRP and CFRP shells containing various core materials. An analytical model was used to describe the static behavior, which shows decent agreement with test results. Initial studies on fatigue characteristics of these strips were carried out as well as tests on associated volute springs. The results contribute to composite lightweight spring design and could extend the range of applications for composite springs in the future.

Index Terms – lightweight design; sandwich structures, static and cyclic torsion

1. INTRODUCTION AND MOTIVATION

Mobility and lightweight construction are currently considered mega trends, which are also addressed for springs and their applications. Many requirements and properties that are important for springs can be realized with fiber-reinforced polymer composites (FRP). The weight-related mechanical properties of laminates can surpass those of metals in the fiber direction and underline the potential for lightweight design. In addition, the optical properties, chemical and corrosion resistance are also advantageous. Furthermore, special areas can be strengthened or weakened locally, according to the function and loads, by adapting the thickness of layers, fiber orientation or material. Since fiber products are often produced as flat textiles, numerous layers would have to be used for thick-walled components. Due to the high material costs and typically low stresses on the inside, sandwich structures can be used for lightweight optimization. Therefore, a low-density core material is placed between the load-bearing cover layers. Figure 1 shows the structure of an FRP sandwich and its implementation on a model aircraft wing. Analogous to large aircraft or wind turbine rotor blades, the sandwich shells have $\pm 45^\circ$ fiber orientation related to the direction of movement, leading to torsional stiffness of the wing. Bending loads are absorbed by the main spar.

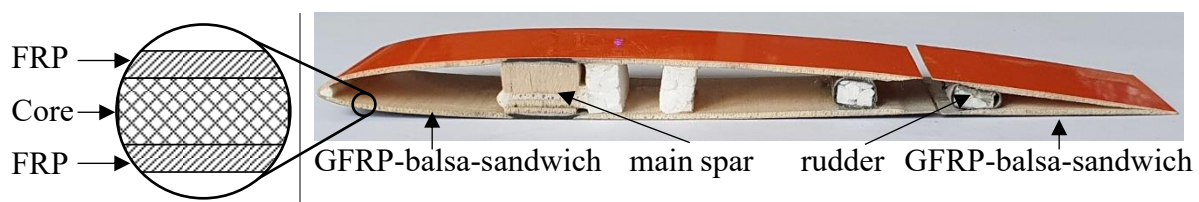


Figure 1. Lightweight optimization through sandwich structures. Left: Schematic; Right: using the example of a cross-section for a model glider (Image: own photo).

Sandwich structures may also be suitable for lightweight springs. However, almost all known FRP springs have full cross sections, because sandwich structures are challenging in design, sensitive in application and particularly vulnerable to cyclic loads. Typical failure modes of sandwich structures are shown in Figure 2.

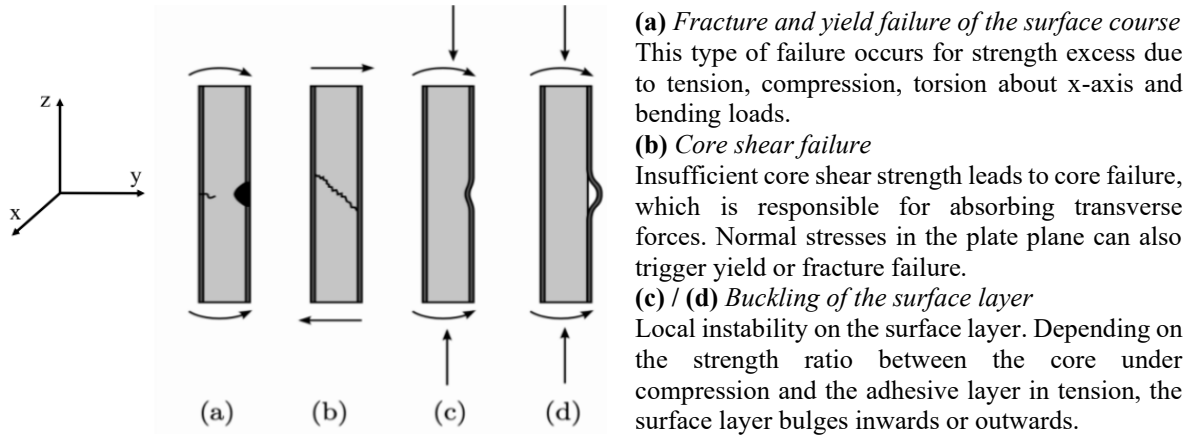


Figure 2. Failure modes of sandwich structures based on [1] [2]

FRP springs have been studied since the 1980s (examples are pictured in Figure 3). From 1981, a transverse leaf spring made of glass fiber (GF) reinforced polymers (GFRP) was installed on the rear axle of the *Chevrolet Corvette C3* (produced 1967-1982), which weighed only about four kilograms and the endurance “was five times longer” [3], compared to their steel counterparts. Leaf springs have become established due to their simple geometry (manufacture) and the main stress (bending stress) running along the spring, which is why the bending strength of unidirectional laminate layers under cyclic loading has already been the subject of scientific investigations [4] [5] [6].

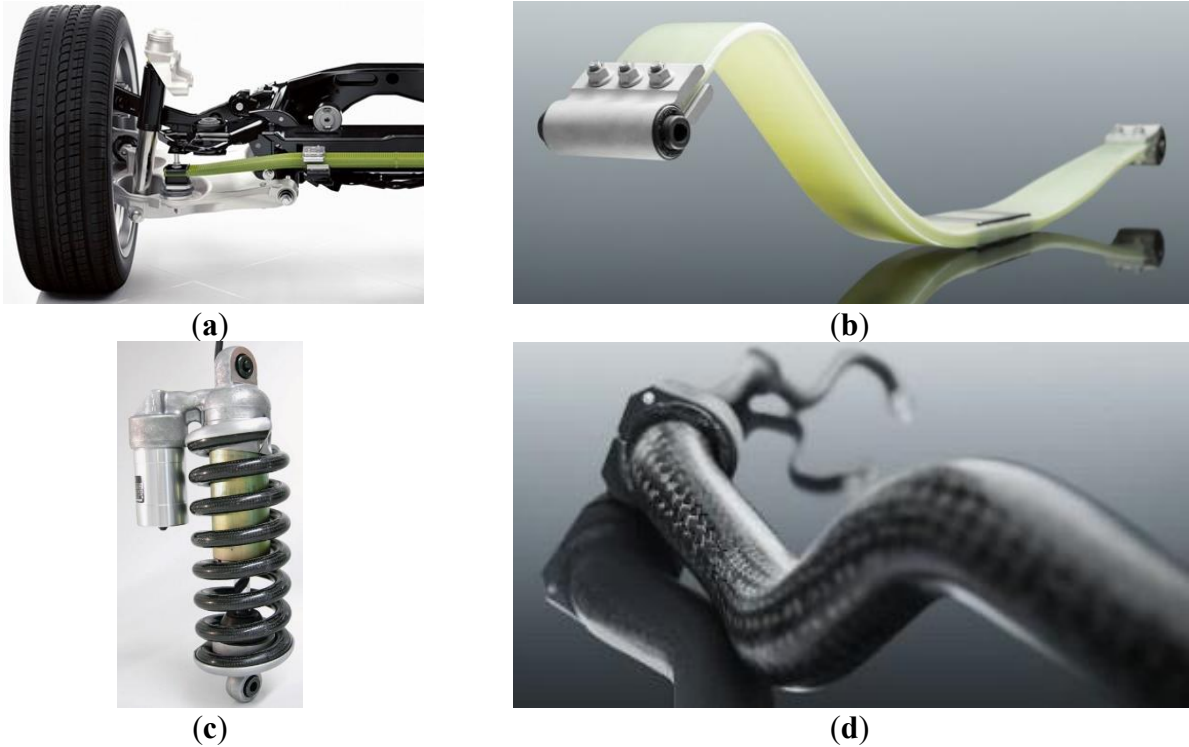


Figure 3. Examples FRP springs. (a) Leaf spring for VOLVO XC90 [7]; (b) MUBEA tension leaf spring [8]; (c) CFRP compression spring [9]; (d) CFRP stabilizer [8]

Concerning other bending loaded springs, further studies were made for tape springs [10], bow springs or C-springs [11][12][13] or ring springs [14]. Based on this, the snail leaf spring was invented [15]. Furthermore, a GFRP tension leaf spring was presented by MUBEA [8][16]. The advantages of free design, e.g. the variable thickness and shape enable an optimal spring design, leading to a weight reduction up to 75% (50 kg/axle) [17][18]. Other bending-loaded FRP springs are meander springs [18][19] or meander spring arrangements like DANTO-springs [20], spiral springs [21][14] and wave spring stacks [22].

In contrast, the composites with round cross-sections have mostly been investigated for torsional loads and used, for example, as stabilizers or helical compression springs. The first known cylindrical laboratory test specimens were manufactured and tested in 1983 with a diameter of 10 mm. Based on this, drive shafts with a diameter of 60 mm were manufactured, which could transmit 280 kNm at 60° rotation until they broke [23][24]. Other torsion springs were examined by [25], [26] and [8], [27] as carbon fiber (CF) vehicle stabilizer springs. A review on helical compression springs was published by [28]. For example, compression spring prototypes were tested in [24], [9] and [29]. For springs with complex stress distribution, e.g. wave spring washers [30], disc springs [9], friction ring springs [30] and bellow springs [9] have been tested.

Apparently, there are already numerous implementations of possible FRP design variants. Springs are often cyclically loaded, so that fatigue properties and failure behavior have to be regarded. For bending-loaded structures and especially for unidirectional (UD) specimens, there are several investigations. Nevertheless, there are uncertainties in mechanical properties that need to be dealt with, as many aspects for springs have not yet received greater attention.

Among the shown composite springs, the conical compression spring, also called volute spring, was developed and analyzed by the authors in the past. It consists of torsional loaded strip material with a rectangular cross-section. As a metal spring, it is rarely used today compared to helical compression springs made of round wires. Associated analyzes and results for torsional loaded plate specimens have already published for static and cyclic characterization by the authors [31]. No investigations are known for torsional loaded sandwich plates and springs, which is why this manuscript shows approaches and results related to this new research field.

2. SANDWICH COMPOSITE TAPE SPRINGS

2.1 Analytical model and FE simulation

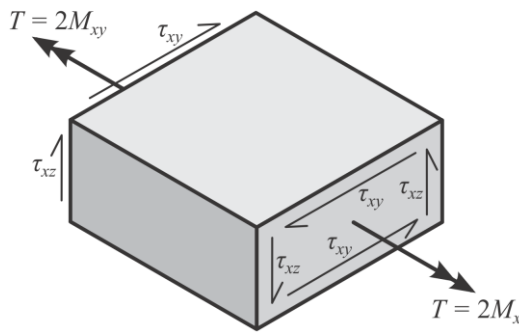
In order to calculate the torsional stiffness of a FRP plate, it is first necessary, to characterize the type of torsion that occurs, distinguishing between pure torsion and free torsion. First of all, pure torsion is defined as a state in which all other degrees of freedom, except the rotation around the longitudinal x-axis, are locked. Consequently, any form of coupling that the laminate exhibits can cause additional stresses, but ultimately only twisting deformations allowed in the laminate. Conversely, free torsion can be defined as a condition in which the only induced load is a torsional moment and all other degrees of freedom are unrestricted. Thus, any form of coupling that the laminate can manifest itself in free torsion as bending, shear or yielding deformation, which occurs as a by-product of the applied torque.

Other scientific papers such as [32][33][34] have also dealt with the torsional stiffness of FRP. However, these do not deal with manufacturing and measurements on sandwich structures.

The calculation of the torsional stiffnesses of the laminate of the different sandwich material combinations was therefore determined using the EXCEL tool ALFALAM (v1.3.1) [35]. This tool is based on the Classical laminate theory according to [36]. A stress-strain-relation of a disc-plate-element can therefore be described by equation (1). [Sch07]

$$\begin{Bmatrix} \{\hat{n}\} \\ \{\hat{m}\} \end{Bmatrix} = \begin{bmatrix} [A] & [B] \\ [B] & [D] \end{bmatrix} \cdot \begin{Bmatrix} \{\varepsilon\} \\ \{\kappa\} \end{Bmatrix} \quad (1)$$

[A] is defined as the stiffness-matrix of the disc-element. [B] is to be seen as a coupling-matrix between disc and plate-element (strain-bending-coupling). Matrix [D] stands for the stiffness-matrix of the plate-element. In particular, the stiffness-matrix of the plate [D] is relevant for the descriptions of the strips. The analytical equation for torsional behavior of a plate element is described by (2) [37]. Figure 4 shows the specific stress distribution for this load case.



$$T = C \frac{d\varphi}{dx} = 2M_{xy} \quad (2)$$

with $C = 4b \cdot D_{66}$

T – Torsional moment
 C – St. Venant torsional stiffness
 x – twisted length
 φ – twist angle
 b – width of specimen
 D_{66} – component of stiffness matrix [D]

Figure 4. Segment of torsional loaded specimen with stress distribution and analytical equation [37]

Additionally, a FE simulation in ANSYS WORKBENCH ACP is used to calculate and evaluate the complex material behavior of the fiber-reinforced sandwich strips for large deformations. The model is based on [Tit19] and [31], but it was modified and extended regarding the sandwich layup. For the surface layers, four UD layers with an alternating $\pm 45^\circ$ fiber orientation made of GFRP or CFRP are applied around the shell body. The core is modeled symmetrically. Thus, the models of the core and surface layer are created and can be transferred as a solid model to the static-mechanical analysis module. Therein, the two solids are connected via a contact condition, resulting in the overall model. In order to simulate the practical torsion tests, one of the two end faces of the strip is fixed and an external displacement is defined on the other side. The degrees of freedom of displacement in the y- and z-direction and the rotation around the y- and z-axis are locked. The displacement in x-direction remains free and a torsion angle around the x-axis is defined as a load. Thus, this load is approximately assumed to be a pure torsional load since four out of six degrees of freedom are locked during the test.

The solution of the static-mechanical analysis resulting from the simulation is passed to the ACP-Post module. The torsional moment-angle of twist characteristics and the failure of the strip can be investigated.

2.2 Sandwich manufacturing and experimental setup

At the beginning, the specimen geometry of the strips must be determined regarding the non-sandwich layup shown in [31]. The specimens with a rectangular cross-section have a length of 250 mm, with 50 mm of each of the two ends clamped during the test. The width was set to 25 mm and the thickness to 1 mm. However, the thickness of the specimens used in this work varies depending on the sandwich material combination. Furthermore, the longitudinal edges have roundings, which are intended to prevent stress peaks/crack initiations during the torsion tests.

In this chapter, a selection of the core materials to be investigated will be made, regarding a suitability test for the volute spring production. Sandwich strips with different core materials were arranged and impregnated with resin. Subsequently, the impregnated tapes were pulled into a shrink tube. For this purpose, common core materials such as Rohacell, CoreCork, glass fiber fleece and balsa wood but also untypical materials such as a precured GFRP and CFRP films were used (Table 1). The fiber orientation of both the balsa wood and the two foils is aligned at 90° to the longitudinal axis of the specimens.

Table 1: Sandwich material combinations used for practical experiments

Surface material	Core material	Abbreviation	Core thickness [mm]
GFRP	-	G	-
	Balsa wood	GB	0.5
	CFRP film	GF	0.2
	Rohacell 51 IG	GR	1.0
	CoreCork NL25	GK	1.0
	Glass fiber fleece	GFF	0.2
CFRP	-	C	-
	Balsa wood	CB	0.5
	CFRP film	CF	0.2
	Rohacell 51 IG	CR	1.0
	CoreCork NL25	CK	1.0
	Glass fiber fleece	GFF	0.2

Due to the manual manufacturing process described above, the shape of the test specimens may deviate from the desired structure, or geometry, and have an influence on the test result. In particular, the thickness can vary, which is why thickness measurement was carried out on all 5 test specimens. This was carried out at all four corners of the measuring range (based on DIN EN ISO 527-5). An overview of the materials investigated is shown in Figure 5.

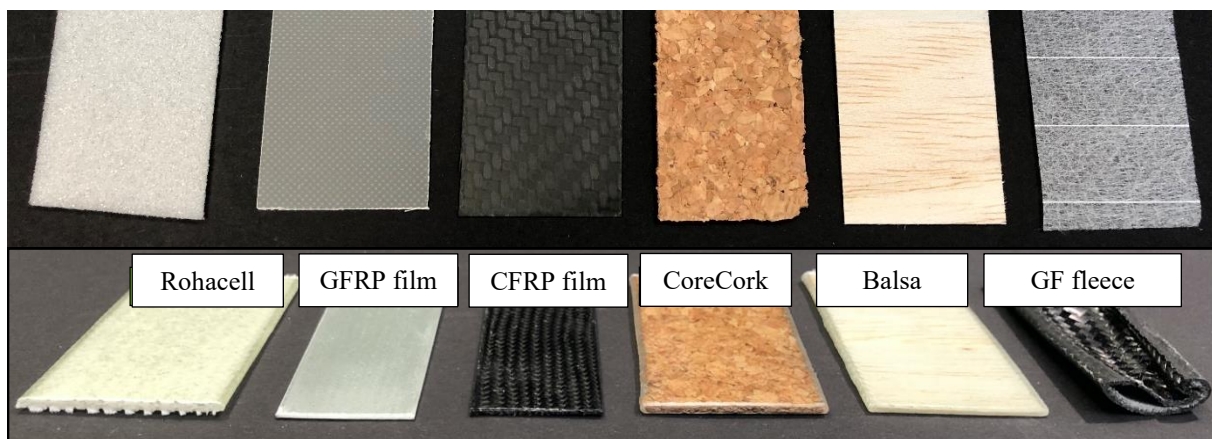


Figure 5. Overview of considered FRP Sandwich combinations. Fleece of glass fibers (right example) is not suitable as core material due to the low thickness, leading to a curvature after shrinking

A further deviation of the structure was found in some specimens with a core layer in the cross-section. Here, the core layer width was too small, and an air channel between the surface and core layers arises. Regarding this issue, there is an increased risk of failure. To avoid the possible influence on the failure behavior, the defective specimens were sorted out.

Due to the transparency of the FRP strips, other visible manufacturing defects can be identified. These include joint defects at the fiber-matrix interface, as well as voids. These defects can cause the specimens to exhibit highly scattering fracture behavior. This can be

influenced by the location and number of defects. A significantly increased number of air inclusions was found in the specimens with a core layer of Rohacell foam.

Additionally, fiber volume content was determined on probes by resin sublimation method through heat exposure (600°C, 30min). The average values for the GFRP specimens are 55.6% and for the CFRP specimens 56.2%.

The torsion tests could be carried out, using the experimental setup shown in Figure 6. A pre-tension force F_{tension} is being applied at the upper clamping to stabilize the test.

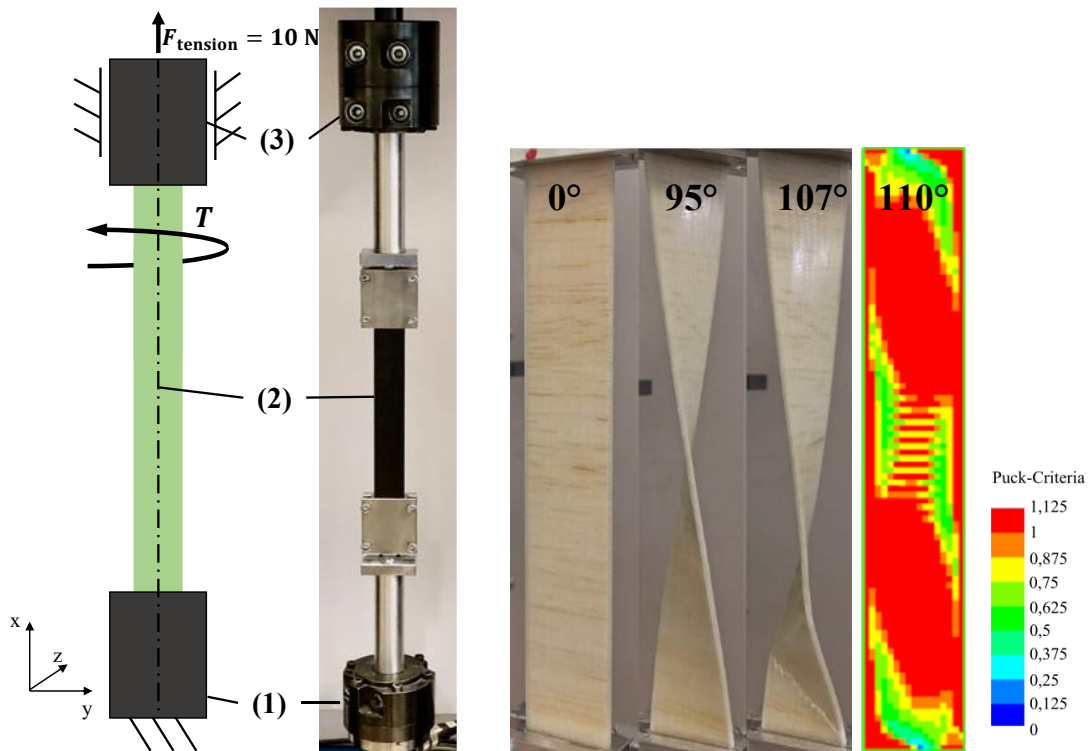


Figure 6. Left: Experimental setup for static torsion tests: (1) Torsional moment sensor / fixated site. (2) Strip specimen. (3) Torque motor site. Middle: Example of torsion test on a GB specimen with characteristic diagonal failure. Right: Associated results of FE simulation shows consistent fracture orientation.

2.3 Results for static loads

To start with the experimental results, a comparison for the analytical and numerical models as well as measurements was carried out for all sandwich combinations (Figure 7). First of all, each three measured curves show decent agreement for the twist angle at first failure at. The simulation agrees very well up to this first fracture of the specimens. However, after the actual fracture of the specimens, the torsional moment of the simulation continues to increase. Possible reasons for this are geometric nonlinearities, which can be caused by large deformation. The deformations result from the twisting, from buckling effects, or from resolved contact conditions. To analyze the failure behavior, the PUCK criterion was defined within ACP Post (see Figure 6 right) and drawn in each diagram. A very good agreement of the failure after PUCK from the simulation with the practical tests is evident.

The analytical method is well applicable for the subjected laminates, but only for smaller twisting angles. Moreover, only the torsional stiffness of the strips can be determined, since it does not include failure criteria. However, for a more precise design of the laminate structures, especially for spring applications, simulations should be used and, in the best case, validated by means of practical tests.

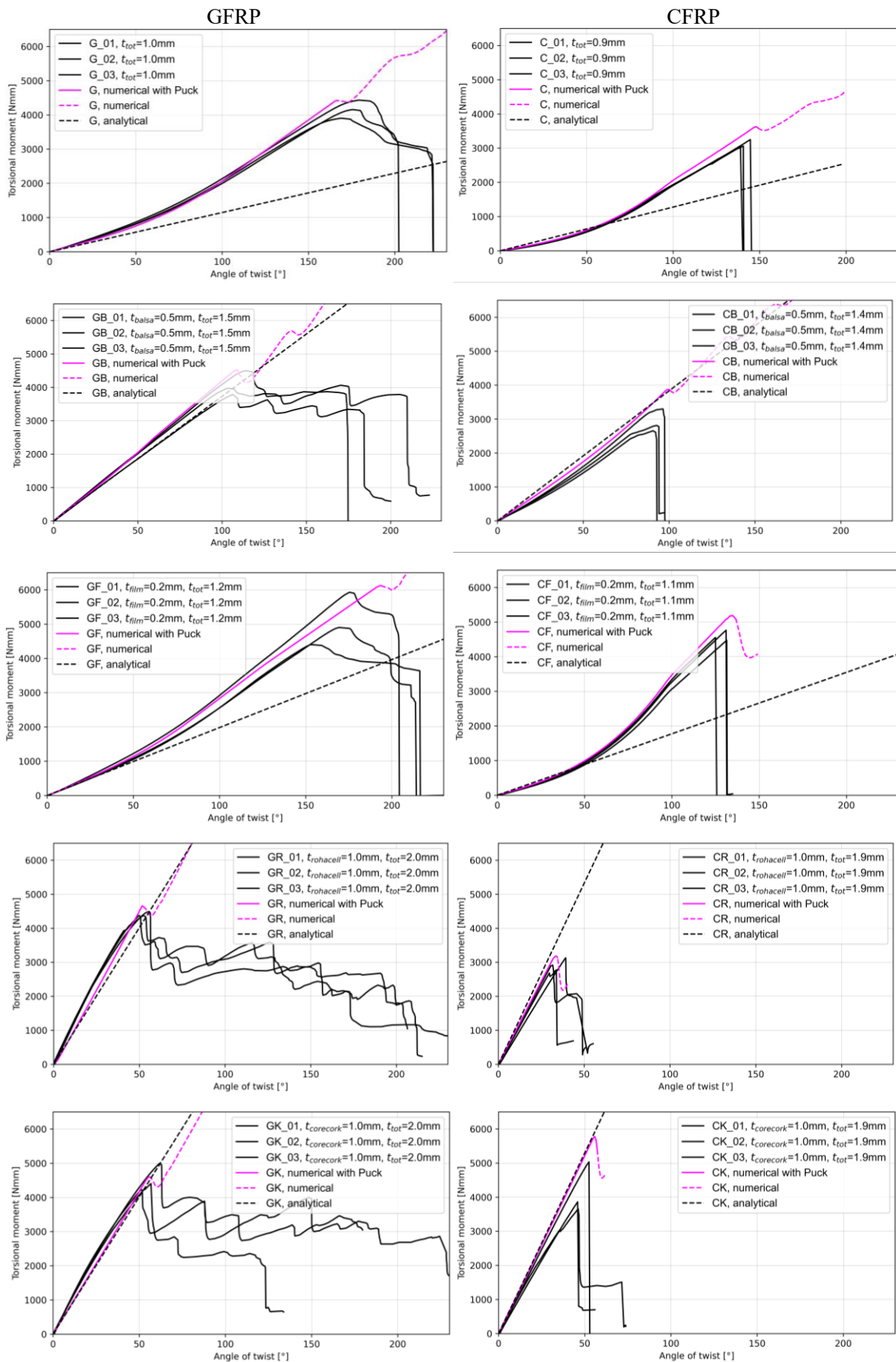


Figure 7. Comparison of analytical and numerical calculations related to measurements for all specimen

This failure analysis was performed for all material combinations, which showed that the analyzed failure always occurred in the area of the first dip of the characteristic curve with a maximum deviation of $\pm 5^\circ$.

Figure 8 displays a comparison of all investigated sandwich materials. On the left side the torsional moment of the GFRP specimen is shown. Compared with the GFRP specimens without a core layer (G and GGG), the sandwich structures show an expected increase in torsional stiffness due to the higher thickness and an increased maximum torsional moment. After reaching the maximum torsional moment, failure occurred in the sandwiched structures (see Figure 6). The fracture behavior at the beginning was analogous to the pure GFRP specimens with buckling, followed by a fracture failure of the outer surface layers. By further load increase, the inner layers and the core layer also failed. As known from literature, a kind fatigue behavior can be stated for all GFRP measurements. After reaching the maximum the first major collapse of the torsional moment by approx. 20-30%, the specimens continue to be loadable and show an intensive degradation behavior until final fracture.

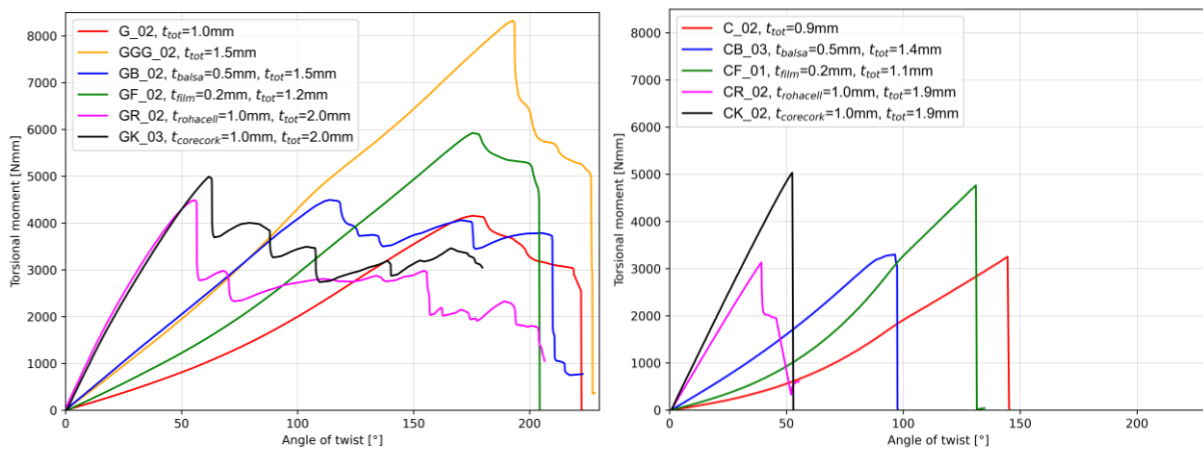


Figure 8. Comparison of torsional characteristics. Left: GFRP sandwiches; Right: CFRP sandwiches

On the right side of Figure 8 all sandwich strips with CFRP surface are displayed (same scaling as the left diagram). Analogous, the CFRP combinations exhibit an increased torsional moment with increasing total thickness. Also, the maximum torsional moment was increased by the use of the sandwich structures. In contrast to the GFRP combinations, there was a simultaneous and impact-induced abrupt failure of the surface and core layers.

This is clearly a difference, compared to GFRP layouts – a fracture occurs suddenly. Therefore, sensible safety factors must be determined when dimensioning CFRP laminates and sandwiches, so that the loads do not reach the area of brittle fracture.

In summary, by using a sandwich structure, both the torsional stiffness as well as the maximum torsional moment could be increased. In addition, the desired property profile can be adapted through the use of different core materials. The material behavior and the limits can be predicted very well by means of a simulation even when a failure criterion is taken into account.

2.4 Results for cyclic loads

Using the same experimental setup on another testing machine, the sandwich strips were then cyclically loaded with pulsating torsion. Figure 9 shows a sequence of emerging fracture on the left side, which leads to a failure at $N = 24,000$ load cycles. On the right side, a detailed view on fracture images for the GB specimen is given. As known from non-sandwich specimen in [31], the stiffness decreases for ongoing load cycles. Therefore, the failure criterion was also linked to the torsional stiffness, and evaluated for stiffness loss of 10%, 20% and 30% regarding the initial value for each specimen.

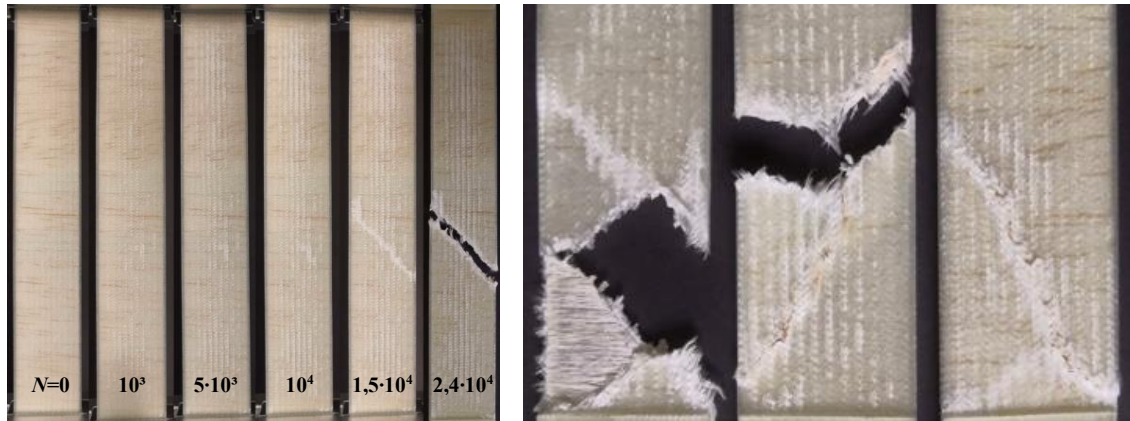


Figure 9. Fracture analyzes of GB specimen. Left: Sequence of emerging fracture over increasing number of load cycles N . Right: detail view on different fracture patterns

Compared with the test results from GFRP strips in [31], the sandwich specimens show more damages over the entire surface. Damage is therefore represented by white areas, where the transparent parts of the FRP become opaque due to micro-damages.

The cyclic tests were carried out for pulsating load, with a mean angle of 50° . In Figure 10 the twist amplitude is plotted against the number of load cycles N (kind of Wöhler diagram). Each black dot marks a total failure of one specimen. Therefore, a Wöhler curve can be calculated, using horizon method. Since the specimens experience a loss of stiffness during the tests, their non-function could be reached earlier. To consider this behavior, the evaluation of a failure was connected to the loss of the torsional moment. Starting with the unloaded specimen, a reduction is stiffness of about 10% occurs for the first load cycles, marked as red dataset. By further load cycles, 20% (green dataset) and 30% (blue dataset) of loss in torsional moment can be determined, leading to the previously described total failure (black dataset).

The same fatigue behavior was determined for the GFRP specimen in [31], but a direct comparison is not possible due to other specimen dimensions and load conditions. Realizing comparability on the basis of stresses and strains is a future task for the authors.

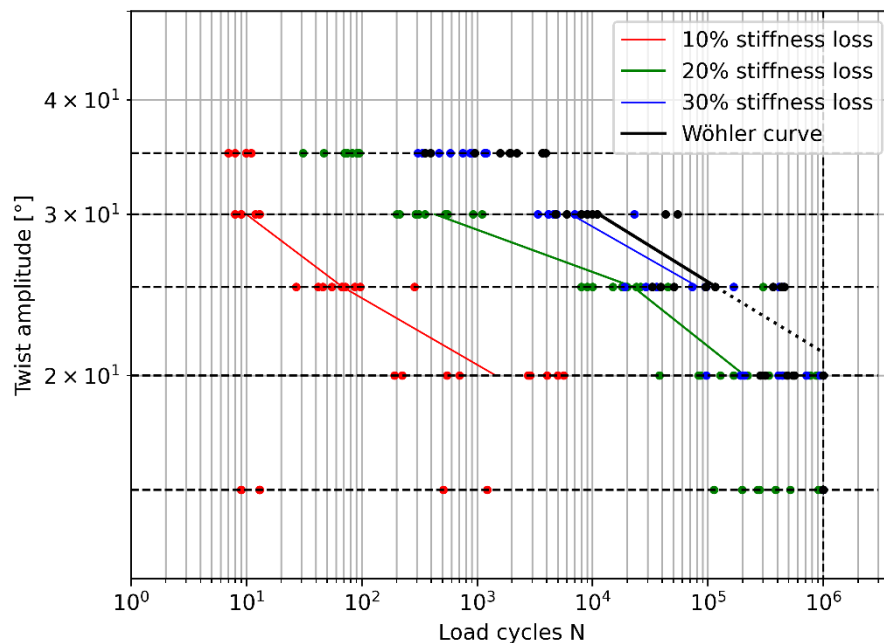


Figure 10. Wöhler-diagram for GB specimen with mean angle of 50° , showing different evaluated stiffness loss. The black dataset regards to total failure of the specimen.

2.5 Sandwich spring manufacturing and qualification

Concluding the research on sandwich strips and springs made out of these materials, this paper uses a two-stage evaluation to recommend a material combination for the volute spring production. In addition, the evaluation shows limits for the use of core materials. Therefore, the mechanical properties of the materials were not in particular of interest, since the initial investigations regarding to manufacturability and general behavior under torsional load. For this purpose, a suitability test of the combinations was carried out, in which one volute spring was produced for each core material. These springs are shown in Figure 11.

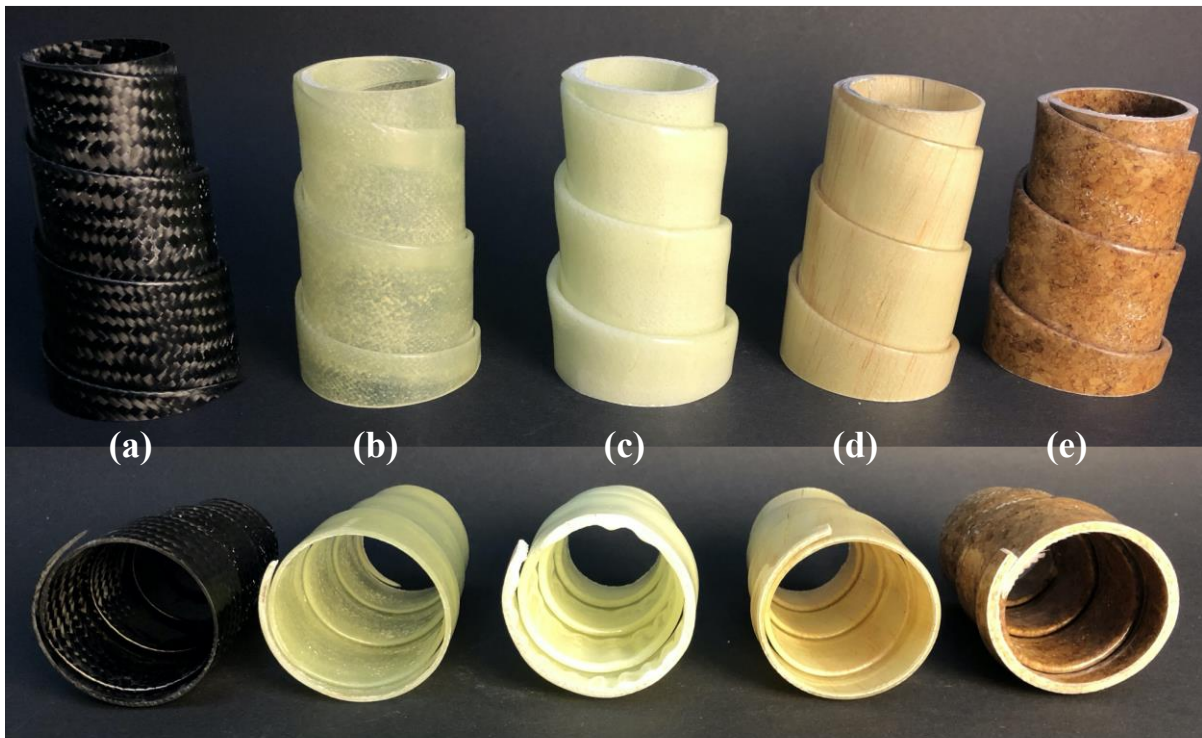


Figure 11. Manufactured volute springs made out of the regarded sandwich materials. (a) CF, (b) GF, (c) GR, (d) GB, (e) GK

For volute spring production, the use of a solid mold would be very complex, due to the typically small distances between the coils. Therefore, the authors developed a production method in the past years, which uses a shrink tube instead of a solid mold. Thus, the resin-impregnated tape is drawn into such a shrink sleeve and shrunk in before winding (disclosed patent application DE102018129530.8 *Method for the production of complex curved structural elements from fiber-reinforced plastics*).

This tube prevents the overlapping layers from bonding with each other during curing. In addition, the shrink tubing serves as a FRP shaping aid. To guarantee the targeted spring geometry, the uncured tape is wrapped around a 3D-printed PLA-shape. This is located inside the spring until the resin is fully cured and is then removed. Finally, the shrink tube can be removed and the spring finish can follow.

Fiber braided sleeves made of CFRP (SILTEX Braided Sleeve 2302) or GFRP (SILTEX Braided Sleeve 1856) are used as semi-finished products for the surface layers, which have a fiber angle of $\pm 45^\circ$ at a width of 25 mm. Due to the wall thickness of the braided sleeves of 0.25 mm, two sleeves are inserted into each other to achieve the total FRP thickness of 1 mm. The core layer is inserted into the two fiber tubes according to the sandwich construction principle. Epoxy resin R&G L285 with hardener H285 is used as matrix material.

After production, the springs were evaluated with respect to their geometric reproducibility (see Figure 11). Basically, it can be seen that the springs with a core layer made of CFRP film (a), GFRP film (b), balsa wood (d) and CoreCork (e) do not exhibit any unacceptable geometrical deviations. In contrast, Rohacell (c), with a thickness of $t = 1.0 \text{ mm}$, showed an unacceptable geometry deviation. This was manifested by strong undulations of the surface on the inner side of the volute spring. In comparison, for example, the CoreCork with the same core layer thickness is suitable. This excludes the Rohacell core material.

Subsequently, evaluation criteria were established and weighted, based on the experiences during manufacturing and properties of core materials (Table 2). The best result is achieved by the GFRP and CFRP film, which is why this core material in combination with a top layer of GFRP or CFRP is recommended as the material combination for volute spring production.

Table 2: Evaluation of core materials for use in lightweight volute springs

Criteria	Weighting	Ideal		Balsa		CoreCork		CFRP-film		GFRP-film	
		p	p·g	p	p·g	p	p·g	p	p·g	p	p·g
A	4	4	16	1	4	2	8	4	16	4	16
B	2	4	8	4	8	1	2	4	8	4	8
C	2	4	8	1	2	2	4	3	6	3	6
D	1	4	4	2	2	1	1	3	3	3	3
E	1	4	4	2	2	2	2	3	3	3	3
Sum		40		18		17		36		36	
Related		100%		45%		43%		90%		90%	
Rank		-		2		3		1		1	

A – handling of core materials during spring production (subjective)

B – dimensional accuracy of the geometry of the core during production

C – mechanical properties of core material

D – production quality of tape specimen

E – core material availability

3. DISCUSSION AND CONCLUSION

In this paper, various combinations of sandwich materials for strips and springs were investigated. For this purpose, a pre-selection of promising core materials was made. These were wrapped with GFRP and CFRP surface layers in strip samples and subjected to static tests. Calculations were carried out with analytical relationships and numerical methods, which generally showed a decent agreement of the torsional moment-twist angle characteristic. However, the analytical relations are sufficiently accurate only for small deformations. FE models with ANSYS ACP show very good agreement of the characteristic curves for all variants. If failure criteria are taken into account, an accurate prediction of the load capacity of the strip specimens is also possible. Additionally, a detailed examination of the manufacturing quality and reproducibility was carried out and points for improvements were identified.

Subsequently, cyclic tests with pulsating torsional loading were carried out for GFRP-balsa strips and showed in principle comparable behavior to the specimens without sandwich core, which were published earlier by the authors. The loss of torsional stiffness should be considered as a failure criterion in relation to the component (spring) function. For example, stiffness losses of 10% were observed after only a few load cycles. This valuable finding should be taken into account for spring designs where a high material utilization is planned. It would be possible to increase the stiffness in the design process compared to the theoretical values so that the desired stiffness is achieved with repeated loads.

Special attention must be paid to the different fracture behavior of GFRP and CFRP. GFRP exhibits a good-natured, successive failure behavior and shows a certain load-bearing

capacity, depending on the advanced degradation. With CFRP, on the other hand, an abrupt, sudden failure of the entire structure can be observed due to the low fracture deformation, which must be taken into account especially for safety components as well as springs.

Finally, volute springs were manufactured from suitable material combinations and the component quality was evaluated. Rohacell (1mm thick) proved to be unsuitable. A comparative evaluation was carried out for the other core materials. Films made of GFRP and CFRP were evaluated best.

For future investigations, it is planned to carry out the calculations and measurements on the basis of stresses and strains for tapes and springs. This will enable a general comparability with literature values and other own investigations. Furthermore, a consideration of cyclic tests on volute springs is to follow in order to apply the findings to concrete components and thus to verify the suitability of the calculations, manufacturing and spring properties.

The contribution provides important results and findings for lightweight springs made of sandwich structures and is intended to support spring designers to approach this complex topic.

REFERENCES

1. *The handbook of sandwich construction*; Zenkert, D., Ed.; Engineering Materials Advisory Services Ltd. (EMAS): Cradley Heath, West Midlands, 1997, ISBN 9780947817961.
2. Gustowski, S. Untersuchung von numerischen Modellierungsverfahren für Verbindungen von Sandwichstrukturen im Flugzeugbau. Masterarbeit; HAW Hamburg, 2016.
3. Wikipedia. Corvette C3. Available online: https://de.wikipedia.org/w/index.php?title=Corvette_C3&oldid=223210149 (accessed on 23 August 2022).
4. Knickrehm, A. Zum Versagen unidirektionaler Glasfaser-Kunststoff-Verbunde bei Biegeschwellbeanspruchung. Dissertation; TU Darmstadt, Darmstadt, 2000.
5. Schoßig, M. *Schädigungsmechanismen in faserverstärkten Kunststoffen: Quasistatische und dynamische Untersuchungen*, 1. Aufl.; Vieweg + Teubner, 2011, ISBN 3834814830.
6. Noël, M. Probabilistic fatigue life modelling of FRP composites for construction. *Construction and Building Materials* 2019, 206, 279–286, doi:10.1016/j.conbuildmat.2019.02.082.
7. Knorra, U. Blattfeder für den Volvo XC90 aus Kunstharz. Available online: <https://www.springerprofessional.de/automobil---motoren/blattfeder-fuer-den-volvo-xc90-aus-kunstharz/6589666> (accessed on 24 August 2022).
8. Muhr und Bender KG. Faserverbundkomponenten: Fahrwerksfedern aus faserverstärkten Kunststoffen. Available online: <https://www.mubea.com/de/faserverbundkomponenten> (accessed on 25 August 2022).
9. Hufenbach, W.; Werner, J.; Körner, I.; Köhler, C. Neuartige Leichtbaufedern in Faserverbundbauweise: Bauweisen / Auslegung / Fertigung. In *Ilmenauer Federntag 2010*, Ilmenau, 2010; STZ Federntechnik, TU Ilmenau, Eds.; ISLE, 2010; Seite 31-44, ISBN 978-3-938843-57-4.
10. Yee, J.; Soykasap, O.; Pellegrino, S. Carbon Fibre Reinforced Plastic Tape Springs. *Proceedings of the 45th AIAA/ASME/ASCE/AHS/ASC Structures, Structural Dynamics, and Materials Conference, Palm Springs, CA 2004*, 19–22.
11. Anastasiades, B. Glass-Reinforced Plastic Springs for Linear Actuators. Semester Project; ETH Zürich, Zürich, 2011.
12. Sardou, M.; Djomseu, P. Composite Compression C Springs & Light Independent Suspension for Trucks, Buses, Cars & Trains. In *SAE Technical Paper Series*. International Truck & Bus Meeting & Exposition, Dec. 04, 2000; SAE International 400 Commonwealth Drive, Warrendale, PA, United States, 2000.
13. Otto Bock Healthcare. C-Walk Prothesenfuß 1C40. Available online: <http://www.ottobock.de/prothetik/produkte-a-bis-z/prothesenfuesse/c-walk/> (accessed on 26 July 2017).
14. Scharr, G. Faserverstärkte Kunststoffe - Federwerkstoffe für den Leichtbau. *VDI-Berichte* 2006, Nr. 1972, 75-86.
15. Michel, S. Schneckenblattfeder. Available online: https://www.innowi.de/media/patente/pdf/HK122_Schneckenblattfeder.pdf (accessed on 25 August 2022).
16. Nowadnick, K. Composite-Blattfeder schlägt Stahlfeder. Available online: <https://industrieanzeiger.industrie.de/top-news/composite-blattfeder-schlaegt-stahlfeder/#slider-intro-2> (accessed on 23 August 2022).
17. Stimpfl, J. Leichtbau in faserverstärktem Kunststoff für Fahrwerksfedern im Automobil. Siegen, April 20, 2016.
18. Kobelev, V.; Alfes, M.; Müller, D. *Meandering axle springs from fibre-reinforced plastic for car suspension: Federn im Fahrzeugbau*, 2015.
19. Rheinmetall AG. Besondere Auszeichnung für neue Glasfaserfeder: Rheinmetall gewinnt den SPE Automotive Award 2022. Available online: https://www.rheinmetall.com/de/rheinmetall_ag/press/news/latest_news/index_35968.php (accessed on 16 February 2023).

20. Brüninghaus, C. Leicht und flexibel: Feder aus glasfaserverstärktem Kunststoff von Danto. *Automobil + Motoren* 2015.
21. Zemann, R. Federleicht. Available online: <https://www.tuwien.at/tu-wien/aktuelles/news/news/federleicht> (accessed on 7 November 2022).
22. *Handbuch Faserverbundkunststoffe/Composites: Grundlagen, Verarbeitung, Anwendungen*; Industrievereinigung Verstärkte Kunststoffe e. V., Ed., 4th ed.; Springer Vieweg: Wiesbaden, 2014, ISBN 978-3-658-02754-4.
23. Sardou, M.; Labbe, T.; Stadler, C. Composit Compression Springs (The Challenger of Helicoidal Springs). In *SAE Technical Paper Series*. International Truck & Bus Meeting & Exposition, Nov. 07, 1994; SAE International400 Commonwealth Drive, Warrendale, PA, United States, 1994.
24. Sardou, M.A. Light weight, Low Cost, Composite Coil Springs are a Reality. Detroit, Michigan (USA), 2005.
25. Puck, A. GFK-Drehrohrfedern sollen höchstbeanspruchte Stahlfedern substituieren. *Kunststoffe* 1990, 80, 1380–1383.
26. Steffens, M. Zur Substitution metallischer Fahrzeug-Strukturbauteile durch innovative Faser-Kunststoff-Verbund-Bauweisen. Dissertation; Universität Kaiserslautern, Kaiserslautern, 2001.
27. Gardiner, G. Converting the structural chassis to composites. *CompositesWorld [Online]*, June 8, 2016. Available online: <https://www.compositesworld.com/articles/converting-the-structural-chassis-to-composites> (accessed on 9 November 2022).
28. Kara, Y. A Review: Fiber Reinforced Polymer Composite Helical Springs. *JOURNAL OF MATERIALS SCIENCE AND NANOTECHNOLOGY* 2017, 5, doi:10.15744/2348-9812.5.101.
29. Automotive Technology. Audi bringt GFK-Feder noch in diesem Jahr in einem Serienmodell. Available online: <https://automotive-technology.de/audi-bringt-gfk-feder-noch-in-diesem-jahr-in-einem-serienmodell/> (accessed on 25 August 2022).
30. Scharr, G. Federn aus Faser-Kunststoff-Verbund. In *KT 2016, Traditio et Innovatio - Entwicklung und Konstruktion*. 14. Gemeinsames Kolloquium Konstruktionstechnik, Rostock, 06.-07.10.2016; Brökel, K., Rieg, F., Stelzer, R.H., Feldhusen, J., Grote, K.-H., Köhler, P., Müller, N., Scharr, G., Eds.; Shaker: Aachen, 2016; pp 146–154.
31. Petrich, M.; Titze, S.; Weimann, T.-L.; Kletzin, U. Examinations on composite strips for springs under torsional load. In *1st Compendium of Modern Spring Technologies 2021*. International Conference on Spring Technologies, Canceled, Nov. 17, 2021; Verband der Deutschen Federnindustrie e.V., Ed.; Hagen, 2021; pp 53–60, ISBN 978-3-00-069928-3.
32. Li, X.; Li, G.; Wang, C.H.; You, M. Optimum Design of Composite Sandwich Structures Subjected to Combined Torsion and Bending Loads. *Appl Compos Mater* 2012, 19, 315–331, doi:10.1007/s10443-011-9204-0.
33. Whitney, J. Stress analysis of laminated, anisotropic plates subjected to torsional loading. In *32nd Structures, Structural Dynamics, and Materials Conference*. 32nd Structures, Structural Dynamics, and Materials Conference, Baltimore, MD, U.S.A., 08 April 1991 - 10 April 1991; American Institute of Aeronautics and Astronautics, Ed.; Reston, Virginia, 1991; 956-962.
34. Rizov, V. Fracture Analysis of Sandwich Beam Loaded in Torsion. *Engineering Mechanics* 2015, 22, 51–58.
35. Weber, T. AlfaLAM - Advanced layerwise failure analysis of Laminates: Berechnungstool zur linearen Laminatanalyse auf Basis der CLT nach der VDI Richtlinie 2014. Available online: https://www.klub.tu-darmstadt.de/forschung_klub/downloads_2/index.de.jsp (accessed on 8 July 2021).
36. Verein Deutscher Ingenieure e.V. *Entwicklung von Bauteilen aus Faser-Kunststoff-Verbund: Berechnungen*, 2006 (2014-3).
37. Honickman, H.; Johrendt, J.; Frise, P. On the torsional stiffness of thick laminated plates. *Journal of Composite Materials* 2014, 2639–2655, doi:10.1177/0021998313501919.

CONTACTS to the Research Group *Wire and Springs* @



Martin Petrich M.Sc.
martin.petrich@tu-ilmenau.de
 Phone: +49 (0) 3677-69-1865



Prof. Dr.-Ing. Ulf Kletzin
ulf.kletzin@tu-ilmenau.de
 Phone: +49 (0) 3677-69-2471